IEEE Access
Multidisciplinary | Rapid Review | Open Access Journal

Received 16 November 2022, accepted 27 November 2022, date of publication 1 December 2022,
date of current version 6 December 2022.

Digital Object Identifier 10.1109/ACCESS.2022.3225879

RESEARCH ARTICLE

Homogeneous Domination-Based Lateral Stability Control Method for Electric Vehicle Lane Keeping System

QIXIAN WANG[1], QINGHUA MENG[1], LIDAN CHEN[2], AND HAIBIN HE[1]
[1]School of Mechanical Engineering, Hangzhou Dianzi University, Hangzhou 310018, China
[2]School of Automotive Technology, Zhejiang Technical Institute of Economics, Hangzhou 310018, China

Corresponding author: Qinghua Meng (mengqinghua@hdu.edu.cn)

This work was supported in part by the Zhejiang Provincial Natural Science Foundation of China under Grant LZ21E050002 and Grant Q22E065759.

ABSTRACT Lane keeping control technology can improve driving safety. But the direct control torque, caused by four in-wheel motors of an electric vehicle driven by four in-wheel motors (EV-DFIM), will affect the vehicle lateral stability. For solving this issue, a two-degree-of-freedom (2DOF) lateral dynamic model of an EV-DFIM lane keeping system is constructed to obtain the lateral stability control state equations. Then a homogeneous domination-based state observer and output feedback controller are designed to improve the vehicle lateral stability and balance when the lane keeping system is working. The Lyapunov method is used to prove that the designed homogeneous domination-based output feedback controller can globally asymptotically stabilize the system. Then, a direct yaw moment strategy is presented based on the optimal allocation algorithm with the lowest utilization rate of the tire to allocate the desired torques for every in-wheel motor. Finally, numerical simulation and HIL simulation are carried out to verify that the proposed lateral stability control method based on homogeneous domination theory for the EV-DFIM lane keeping system has a good control effect and robustness.

INDEX TERMS Electric vehicle driven by four in-wheel motors, homogeneous domination control, nonlinear control, vehicle dynamics, vehicle stability.

I. INTRODUCTION

Thanks to the development of control technology, sensor technology and computer technology, intelligent driving has become a research hotspot. As a basic function of L1 level automatic driving technique, lane keeping assistance system (LKA) has become mature and is widely used which improves the driving safety obviously. Many researchers have proposed some achievements. For example, H. Wang et al. proposed a control method combining the extension control and Takagi-Sugeno-Kang fuzzy control for lane keeping system control to solve a single control algorithm resulting in poor control effect [1]. M. Karthikeyan et al. used a machine learning algorithm in the LKA system for accident-free driving of autonomous vehicles [2]. However, previous studies on LKA system did not consider the vehicle lateral stability when the LKA system is working. For a traditional vehicle, the motor of the electronic power steering system (EPS) is used as the actuator of the LKA. The controller controls the motor to drive the steering system to actively correct the driving direction. If the vehicle deviates from the desired lane obviously when suffers external disturbances suddenly under high speed, the actuator of LKA will forces the steering gear to output an inverse steering angle immediately that may cause the trail-swing and sideslip phenomena. The two phenomena are unstable and dangerous. For an EV-DFIM, the in-wheel motor's torque directly acts on the wheels with high transmission efficiency. By changing the driving torques of the in-wheel motors, active braking control, electronic stability control and the adaptive cruise control can be carried out conveniently. Therefore, the EV-DFIM has good development in the future [3], [4], [5], [6], [7]. The EV-DFIM has

The associate editor coordinating the review of this manuscript and approving it for publication was Christopher H. T. Lee.

precise and flexible torque response, superior performance in dynamic performance and handling activity, which makes it easier to adopt lane keeping technology. But it is also easy to affect the vehicle stability when the lane keeping system is working. Some researchers studied the vehicle lateral stability control problem, but they did not consider the influence of LKA system. For example, S. Ding et al. designed a direct yaw moment lateral stability control method for four-wheel driving electric vehicles by finite-time control method [8]. Z. Zhao et al. proposed a joint control strategy that combined linear programming algorithm combining exponential reaching law with saturation function and improved sliding mode algorithm to solve the instability phenomenon caused by differences among four driving wheels [9]. E. Joa proposed a four-wheel independent brake control method for vehicle stability under various road conditions without any tire-road friction information, which can guarantee vehicle stability under unknown road conditions [10]. Considering uncertain external disturbance due to the frequent variation of running conditions, X. He et al. proposed a novel robust coordination control strategy for the active front steering (AFS) system and active rear steering (ARS) system to simultaneously suppress lateral path tracking deviation while keeping autonomous vehicle stability under dynamic driving situations under handling limit [11]. A simultaneous path following and lateral stability control method was presented by T. Chen et al. for four-wheel independent drive and four-wheel independent steering (4WD-4WS) autonomous electric vehicles based on Hamilton energy function with the actuator saturation [12]. To further improve the handling stability of four-wheel independent driving electric vehicles, C. Zhang et al. designed a controller with a layered structure with the upper controller based on fuzzy control and the lower controller based on regular allocation strategy and proved the effectiveness of the controller through simulation experiments [13]. A. T. Nguyen et al. designed a new LPV static output feedback controller to improve the lateral stability and the driving comfort of the narrow tilting vehicles without vehicle sensors [14]. Z. Li et al. proposed a model predictive controller for the EV-DFIM under extreme driving situations [15]. C. Q. Jing et al. presented a novel integrated control strategy of yaw stability and energy efficiency based on model predictive control and active steering system. The integrated control method can improve energy efficiency [16]. Meng et al. studied the stability of the EV-DFIM and proposed lateral stability control methods based on the sampled-data control method and direct yaw moment respectively [17], [18].

The aforementioned vehicle stability control methods require that the state equations of vehicle stability control systems strictly meet linear growth, which is difficult for the control system state equations based on the vehicle dynamics model. In recent years, a homogeneous domination method has been developed [19], [20], [21]. This method has strong robustness, reduces the strict limitation for linear growth of the state equation, and is more suitable for engineering applications. Although there are many design methods and ideas for the controller, it ultimately boils down to state feedback and output feedback. For output feedback control dependent on the observer theory, most of the existing methods are based on linear-like observers, which may not be suitable for handling highly nonlinear functions. A homogeneous system means that the vector field describing the control system is homogeneous. The homogeneity of the vector field ensures that there is a mapping relationship between the solution space and the unit closed ball in the solution space, so the whole solution space can be regarded as the expansion of the unit closed ball. It shows that the locally asymptotically stably autonomous system is also globally asymptotically stable. Therefore, the global stability problem of homogeneous systems can come down to its local stability problem. The stability of a homogeneous system can be characterized by homogeneity, so the system stability can be analyzed by using the relation between homogeneity and stability. If the vector field corresponding to a stable homogeneous system can be decomposed into a sum of several homogeneous vector fields, then the original vector field is also asymptotically stable if the vector field which has minimal homogeneity is asymptotically stable. Further, it can be concluded that a stable homogeneous system coupled with a higher-order perturbation term still is stable. When a homogeneous system adds an integrator, the system can still be stabilized by homogeneous feedback. Therefore, the homogeneous control method provides a new design approach to solve the global stabilization of uncertain nonlinear systems, allowing us to construct the global output feedback controllers under weak growth conditions. The controller constructed by this control method can control uncertain nonlinear terms whose precise information is unknown. Qian proposed a homogeneous domination approach for the global output feedback stabilization of nonlinear systems firstly in paper [22]. He and his followers developed the homogeneous domination control method for many nonlinear systems [23], [24], [25], [26], [27], [28], [29]. Other researchers also developed this method. To globally stabilize the p-normal form nonlinear system with unknown power integrators, G. Zhao et al. constructed a state-dependent homogeneous domination stabilizer [30]. For a class of high-order switched nonlinear systems with quantized input, Y. Jiang et al. designed a homogeneous output feedback controller to ensure global boundedness of all the states in the whole system and the tracking error to converge into an arbitrarily small neighborhood of origin in finite time [31]. For stochastic high-order time-delay switched nonlinear systems, A. Lx et.al constructed an output tracking controller under arbitrary switching to guarantee that the tracking error can be tuned small enough in the mean-square sense while all states of the closed-loop system remain to be bounded in probability [32]. K. Alimhan et al. proposed an output feedback tracking controller by using a homogeneous domination method for a class of high-order nonlinear systems with time delay [33]. With the help of homogeneous domination, Liu et al. designed an output-feedback

control scheme for a class of stochastic nonlinear systems with time-varying powers and it can be proved to be globally asymptotically stable [34]. Liu et al. proposed an adaptive homogeneous domination method for time-varying control of nonlinear systems [35]. Meng et al. proposed a homogeneous output feedback control method for the active suspension of an intelligent electric vehicle [29]. Sun et al. proposed an output feedback controller that can deal with unknown measurement sensitivity based on the homogeneous dominance technique [36].

In this paper, we will solve the lateral stability issue of the EV-DFIM LKA system via the homogeneous domination control method. Based on the homogeneous theory, a homogeneous domination-based control method is proposed to ensure the lateral stability of the EV-DFIM LKA system when the vehicle suffers uncertain disturbance caused by road profile, lateral wind, and different tire pressure during vehicle driving. The main contributions of this paper are as follows.

- Via coordinate transformation for the control system state equations, a domination gain is introduced into the control system to amplify the effect of the controller and suppress the negative effects of nonlinear items.
- A homogeneous domination state observer and controller are designed for the lateral stability of an EV-DFIM LKA system based on the homogeneous theory. The proposed homogeneous domination-based control method does not require the unknown and nonlinear items of the control system to meet the strict linear growth.
- The hardware-in-loop simulation is carried out by using the driverless car designed by ourselves to verify the effectiveness of the homogeneous domination controller.

The rest of the paper is organized as follows. The 2DOF lane-keeping tracking error model is constructed in section II. Then the homogeneous domination-based state observer and controller are designed in section III. A yaw moment distribution strategy is presented in section IV. Numerical and HIL Simulations are carried out to verify the effectiveness of the proposed method in section V and VI respectively. Finally, the conclusion is given in section VII.

II. CONSTRUCTION OF LATERAL DYNAMICS MODEL FOR EV-DFIM LKA SYSTEM

To reduce the difficulty of developing a lateral stability control method for an EV-DFIM LKA system, we simplify the EV-DFIM to a 2DOF model in this paper, as shown in Figure 1. Although the model is identical to a conventional engine vehicle, the difference is that each wheel of the EV-DFIM is independently driven by an in-wheel motor. Due to the fast and accurate torque response of the motor, it is easy to generate an additional torque M_z to adjust the lateral motion of the vehicle. In order to design an effective controller, roll and pitch motion are ignored during modeling. The ideal lateral dynamics mathematical

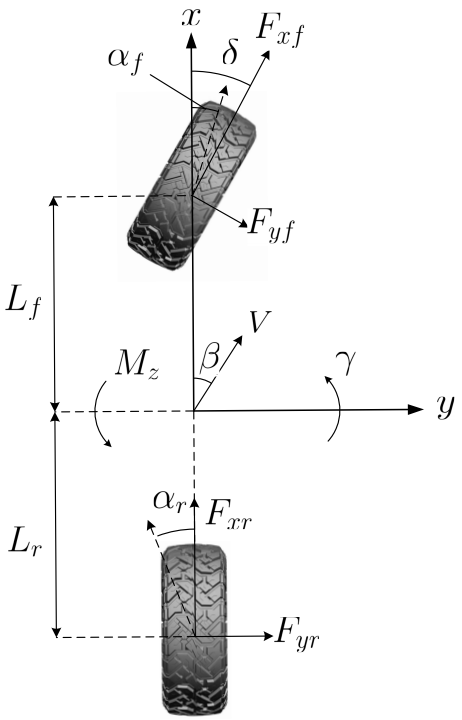

FIGURE 1. Two-degree-of-freedom Model for an EV-DFIM LKA system.

model is expressed below.

$$\begin{aligned}\dot{\beta}_d &= \frac{F_{yf}+F_{yr}}{mv_x} - \gamma_d \\ \dot{\gamma}_d &= \frac{L_f F_{yf} - L_r F_{yr} + M_{zd}}{I_z},\end{aligned} \tag{1}$$

where β_d is the ideal side slip angle of vehicle centroid, γ_d is the ideal yaw rate, F_{yf} and F_{yr} are the lateral forces of front and rear wheels respectively, v_x is the longitudinal velocity, m and I_z are the mass and moment of inertia respectively, L_f and L_r are the distance between the front axle and centroid and the distance between the rear axle and centroid respectively, M_{zd} is the ideal additional yaw moment.

In this paper, the linear front and rear tire lateral forces are calculated as [37]

$$F_{yf} = C_f\alpha_f, F_{yr} = C_r\alpha_r, \tag{2}$$

where C_f and C_r are equivalent lateral stiffnesses of the front wheel and rear wheel respectively. α_f and α_r are their wheel side slip angles respectively which are calculated by

$$\begin{aligned}\alpha_f &= -(\beta_d + \frac{L_f\gamma_d}{v_x} - \delta(t)) \\ \alpha_r &= -(\beta_d - \frac{L_r\gamma_d}{v_x}),\end{aligned} \tag{3}$$

where $\delta(t)$ is the time-varying front wheel steering angle. According to Eq.2 and Eq.3, the system (1) can be expressed as

$$\dot{\beta}_d = -\frac{(C_f+C_r)\beta_d}{mv_x} + \frac{(C_rL_r - C_fL_f)\gamma_d}{mv_x^2} - \gamma_d$$

$$+\frac{C_f}{mv_x}\delta(t)$$
$$\dot{\gamma}_d = \frac{(C_rL_r - C_fL_f)\beta_d}{I_z} - \frac{(C_fL_f^2 + C_rL_r^2)\gamma_d}{I_zv_x} + \frac{M_{zd}}{I_z} + \frac{C_fL_f}{I_z}\delta(t). \quad (4)$$

In actual working conditions, an EV will be interfered by many external factors. Therefore, the actual 2-DOF electric vehicle model can be expressed as

$$\dot{\beta}_p = -\frac{(C_f + C_r)\beta_p}{mv_x} + \frac{(C_rL_r - C_fL_f)\gamma_p}{mv_x^2} - \gamma_p + \frac{C_f}{mv_x}(\delta(t) + \Delta\delta(t))$$
$$\dot{\gamma}_p = \frac{(C_rL_r - C_fL_f)\beta_p}{I_z} - \frac{(C_fL_f^2 + C_rL_r^2)\gamma_p}{I_zv_x} + \frac{M_{zd}}{I_z} + \frac{C_fL_f}{I_z}(\delta(t) + \Delta\delta(t)), \quad (5)$$

where β_p is the actual side slip angle, γ_p is the actual yaw rate, $\Delta\delta(t)$ is the uncertain disturbance caused by road profile, lateral wind, and different tire pressure during vehicle driving, M_{zp} is the actual additional yaw moment. To simplify the analysis, researchers generally treat the speed v_x as a constant. In fact, the vehicle speed is time-varying. To reflect the actual situation, this paper considers v_x to be time-varying. For convenience, v_x is expressed in the following form.

$$\rho_1(t) = \frac{1}{v_x}, \rho_2(t) = \frac{1}{v_x^2}. \quad (6)$$

Although v_x is time-varying, it still has a maximum value. Therefore,

$$\rho_1(t) \le \theta_1, \rho_2(t) \le \theta_2, \rho_1(t) > 0, \rho_2(t) > 0. \quad (7)$$

Based on Eq.4 and Eq.5, one can obtain

$$\dot{e}_\beta = -\frac{(C_f + C_r)e_\beta}{mv_x} + \frac{(C_rL_r - C_fL_f)e_\gamma}{mv_x^2} - e_\gamma + \frac{C_f}{mv_x}\Delta\delta(t)$$
$$\dot{e}_\gamma = \frac{(C_rL_r - C_fL_f)e_\beta}{I_z} - \frac{(C_fL_f^2 + C_rL_r^2)e_\gamma}{I_zv_x} + \frac{\Delta M_z}{I_z} + \frac{C_fL_f}{I_z}\Delta\delta(t), \quad (8)$$

where $\dot{e}_\beta = \dot{\beta}_p - \dot{\beta}_d$, $\dot{e}_\gamma = \dot{\gamma}_p - \dot{\gamma}_d$, $e_\beta = \beta_p - \beta_d$, $e_\gamma = \gamma_p - \gamma_d$. $\Delta M_z = M_{zp} - M_{zd}$ is the additional torque which is necessary to keep the electric vehicle stable.

Denote $x(t) = (x_1(t), x_2(t))^T \in \mathbb{R}^2$, $u(t) \in \mathbb{R}$, $y(t) \in \mathbb{R}$, and $d(t) \in \mathbb{R}$. They are the state variables, controller, system output, and uncertain disturbance of the system respectively. Define

$$x_1(t) = e_\beta,$$
$$x_2(t) = \frac{(C_rL_r - C_fL_f)\rho_2(t) - m}{m}e_\gamma,$$
$$u(t) = \frac{(C_rL_r - C_fL_f)\rho_2(t) - m}{mI_z}\Delta M_z,$$
$$d(t) = \Delta\delta(t).$$

Then Eq.8 can be rewritten as

$$\dot{x}_1(t) = x_2(t) + \phi_1(t, x(t))$$
$$\dot{x}_2(t) = u(t) + \phi_2(t, x(t))$$
$$y(t) = x_1(t), \quad (9)$$

where

$$\phi_1(t, x(t)) = -\frac{(C_r + C_f)}{m}\rho_1(t)x_1(t) + g_1d(t),$$
$$\phi_2(t, x(t)) = \frac{[(C_rL_r - C_fL_f)\rho_2(t) - m]}{mI_z} \times (C_rL_r - C_fL_f)x_1(t) + \left[-\frac{C_rL_r^2 + C_fL_f^2}{I_z} \times \rho_1(t) + \frac{(C_rL_r - C_fL_f)\dot{\rho}_2(t)}{(C_rL_r - C_fL_f)\rho_2(t) - m}\right]x_2(t) + g_2d(t),$$
$$g_1(t) = \frac{C_f}{m}\rho_1(t),$$
$$g_2(t) = \frac{(C_rL_r - C_fL_f)\rho_2(t) - m}{m}\frac{C_fL_f}{I_z}.$$

III. DESIGN OF HOMOGENEOUS DOMINANT-BASED OBSERVER AND CONTROLLER

The research achievement of this paper is expressed by Theorem 1. The Theorem 1 is presented based on the Assumption 1.

Assumption 1: There exist $\tau \ge 0$ and $c \ge 0$ such that the unknown nonlinear terms of the control system enable

$$|\phi_i| \le c(|x_1|^{\frac{i\tau+1}{}} + \cdots + |x_i|^{r_i}), \quad i = 1, 2, \quad (10)$$

where $r_i = \frac{i\tau+1}{(i-1)\tau+1}$.

Theorem 1: Under Assumption 1, the homogeneous domination-based observer (11) and controller (12) are designed to render system (9) globally asymptotically stable.

$$\hat{x}_1 = x_1$$
$$\hat{x}_2 = (\eta_2 + n_1\hat{x}_1)^{h_1}$$
$$\dot{\eta}_2 = -m_1\hat{x}_2, \quad (11)$$

where $h_1 > 0, m_1 > 0, n_1 > 0$.

$$u(\hat{x}) = -\gamma_2(\hat{x}_2 + \hat{x}_1^{p_1}\gamma_1)^{h_2}$$
$$h_1 = l_2/l_1$$
$$h_2 = (l_2 + \tau)/l_2, \quad (12)$$

where γ_i is a constant, l_i is the homogeneous weight of x_i, τ is the homogeneous degree of the designed controller.

Remark 1: The side slip angle β can be obtained by longitudinal velocity and lateral velocity via two sensors. The longitudinal velocity can be measured by a sensor mounted on the transmission output shaft, and the lateral velocity can

be obtained by a lateral acceleration sensor. The two sensors have already been used in a vehicle. It does not need to add new sensors and modify the vehicle circuit for the cost. Therefore, x_2 (e_γ) will be estimated by the designed observer.

We first give some important lemmas about homogeneous theory and inequalities which will be used in the proof.

Lemma 1 ([38] Weighted Homogenity): For a selected coordinates $(x_1, x_2, \cdots, x_n) \in \mathbb{R}^n$ and real numbers $r_1, r_2, \cdots, r_n$, where $r_i > 0$,

- Dilation $\Delta_\varepsilon(x)$ is defined as

$$\Delta_\varepsilon(x) = (\varepsilon^{r_1}x_1, \varepsilon^{r_2}x_2, \cdots, \varepsilon^{r_n}x_n), \forall \varepsilon > 0,$$

  where r_i are called as the weights of the coordinations.
- A function $V \in C(\mathbb{R}^n, \mathbb{R})$ is homogeneous of degree τ if there exists a $\tau \in \mathbb{R}$, then $\forall x \in \mathbb{R}^n \setminus 0, \varepsilon > 0, V(\Delta_\varepsilon(x)) = \varepsilon^\tau V(x_1, x_2, \cdots, x_n)$.
- A vector field $f \in C(\mathbb{R}^n, \mathbb{R}^n)$ is considered to be homogeneous of degree τ if there exists a $\tau \in \mathbb{R}$, then $\forall x \in \mathbb{R}^n \setminus 0, \varepsilon > 0, f_i(\Delta_\varepsilon(x)) = \varepsilon^{\tau+r_i} f_i(x)$.
- A homogeneous p-norm is defined as

$$\|x\|_{\Delta_\varepsilon, p} = \left(\sum_{i=1}^{n} |x_i|^{\frac{p}{r_i}}\right)^{\frac{1}{p}}, \forall x \in \mathbb{R}^n, \tag{13}$$

  where p is a constant and $p \geq 1$.

Lemma 2 [39]: If V_1 and V_2 are homogeneous functions of degree τ_1 and τ_2 having a same dilation weight $\Delta = (r_1, r_2, \cdots, r_n)$, the homogeneous degree of $V_1 \cdot V_2$ is $\tau_1 + \tau_2$ with respect to the same dilation weight.

Lemma 3 [39]: Suppose $V : \mathbb{R}^n \longrightarrow \mathbb{R}$ is a homogeneous function of degree τ with respect to a given dilation weight $\Delta = (r_1, \cdots, r_n)$. Then the following items hold.

- $\partial V / \partial x_i$ is homogeneous of degree $\tau - r_i$ with respect to the dilation weight Δ.
- There is a positive constant w_1 to ensure $V(x) \leq w_1 \|x\|_\Delta^\tau$.
- If $V(x)$ is positive definite, there is a positive constant w_2 to ensure $w_2 \|x\|_\Delta^\tau \leq V(x)$.

Lemma 4 [40]: when $x \in \mathbb{R}, y \in \mathbb{R}, p \geq 1$, the following inequalities hold.

$$|x + y|^p \leq 2^{p-1}|x^p + y^p|, \tag{14}$$
$$(|x| + |y|)^{1/p} \leq |x|^{1/p} + |y|^{1/p}. \tag{15}$$

if $p \geq 1$ is odd function, then

$$|x - y|^p \leq 2^{p-1}|x^p - y^p|. \tag{16}$$

Lemma 5 [41]: when c, d are constant, then

$$|x|^c|y|^d \leq \frac{c}{c+d}\gamma|x|^{c+d} + \frac{d}{c+d}\gamma^{-c/d}|y|^{c+d}. \tag{17}$$

Lemma 6 [41]: Let $p \geq 1$ be an odd real number, the following inequality holds.

$$|x^p - y^p| \leq p|x - y|(x^{p-1} + y^{p-1}). \tag{18}$$

Next we use Lyapunov method to prove Theorem 1.

Proof

we first prove that the designed homogeneousdomination-based state feedback controller can stabilize system (19) which does not include the unknown nonlinear items.

$$\begin{aligned} \dot{x}_1 &= x_2 \\ \dot{x}_2 &= u. \end{aligned} \tag{19}$$

Define $u := x_3 \in \mathbb{R}$, and $y := x_1 \in \mathbb{R}$. Select equation $V_1(x_1) = \frac{l_1}{2l_2 - \tau} x_1^{\frac{2l_2-\tau}{l_1}}$. Defining a virtual controller $x_2{}^*$, $x_2{}^* = -x_1^{l_2/l_1}\alpha_1, \alpha_1 = 2 + c, \xi_i = x_i - x_i^*, i = 1, 2$, the derivative of $V_1(x_1, x_2)$ is

$$\dot{V}_1(x_1, x_2) \leq -2x_1^{\frac{2l_2}{l_1}} + x_1^{\frac{2l_2-\tau}{l_1-1}}(x_2 - x_2{}^*). \tag{20}$$

Constructing Lyapunov function

$$V_2(x_1, x_2) = V_1 + \frac{l_2}{2l_2 - \tau}\xi_2^{\frac{2l_2-\tau}{l_2}}, \tag{21}$$

the derivative of lyapunov function $V_2(x_1, x_2)$ is

$$\begin{aligned} \dot{V}_2(x_1, x_2) \leq &-2\xi_1^{2l_2/l_1} + \xi_1^{\frac{2l_2-\tau}{l_1}-1}\xi_2 \\ &+\xi_2^{\frac{2l_2-\tau}{l_2}-1}(x_3 + \phi_2(x) - \frac{\partial x_1{}^*}{\partial x_1}\dot{x}_1). \end{aligned} \tag{22}$$

According to the form of the virtual controller defined earlier, there exists

$$x_3^* = -\alpha_2\xi_2^{\frac{l_3}{l_2}} = -(1 + c_2 + \hat{c}_2)\xi_2^{\frac{l_3}{l_2}}, \tag{23}$$

where $\alpha_2 > 0$.

Th state feedback controller can be defined as

$$u = x_3^* = -\alpha_2\xi_2^{\frac{l_2+\tau}{l_2}}. \tag{24}$$

Therefore, there is

$$\dot{V}_2 \leq -(\xi_1^{\frac{2l_2}{l_1}} + \xi_2^2) + \xi_2^{\frac{2l_2-\tau}{l_2}-1}(u - u^*). \tag{25}$$

It is obvious that $\dot{V}_2$ is a negative definite function, which proves that the state feedback controller can globally asymptotically stabilize system (19).

Next, we will prove that the state feedback controller can stabilize the lateral stability control system of the EV-DFIM (9).

Select

$$u^* = -\alpha_2\xi_2^{\frac{l_2+\tau}{l_2}}. \tag{26}$$

Then there is

$$\dot{V}_2 \leq -\xi_1^{2l_2/l_1} - \xi_2^{2l_2/l_2} + \frac{\partial V_2(x_2)}{\partial x_1}\phi_1(x) + \frac{\partial V_2(x_2)}{\partial x_2}\phi_2(x). \tag{27}$$

According to Assumption 1, there exist

$$\begin{aligned} \phi_1(t, x_1) &\leq c(|x_1|^{\tau+1}, \\ \phi_2(t, x_1, x_2) &\leq c(|x_1|^{\tau+1} + |x_2|^{\frac{2\tau+1}{\tau+1}}). \end{aligned} \tag{28}$$

Therefore (27) is rewritten as

$$\begin{aligned}\dot{V}_2 &\leq -\xi_1^{2l_2/l_1}+\xi_2^2+2\overline{\kappa}(\xi_1^{2l_2/l_1}+\xi_2^2)\\ &< -(\xi_1^{2l_2/l_1}+\xi_2^2)(1-2\overline{\kappa}).\end{aligned} \tag{29}$$

It is concluded that there is a $\overline{\kappa}$ to make $\dot{V}_2 < 0$, i.e., the designed state controller can stabilize system (9).

The following work is to prove that the designed observer and controller can globally asymptotically stabilize system (9).

Similar to the previous proof, we first prove that the system (19) can be stabilized by the designed controller and observer.

Construct a C^1 function

$$U_2=\int_{(\eta_2+m_1x_1)^{\frac{l_2}{l_1}}}^{x_2}(s^{\frac{l_1}{l_2}}-(\eta_2+m_1x_1))ds. \tag{30}$$

Then the following formula can be obtained.

$$\begin{aligned}\frac{\partial U_2}{\partial x_1}&=-m_1(x_2-(\eta_2+m_1x_1)^{\frac{l_2}{l_1}}),\\ \frac{\partial U_2}{\partial x_2}&=(x_2^{\frac{l_1}{l_2}}-(\eta_2+m_1x_1)),\\ \frac{\partial U_2}{\partial \eta_2}&=-(x_2-(\eta_2+m_1x_1)^{\frac{l_2}{l_1}}).\end{aligned} \tag{31}$$

Therefore, the derivative of U_2 is

$$\begin{aligned}\dot{U}_2=u(\hat{x})(x_2^{\frac{l_1}{l_2}}&-(\eta_2+m_1x_1))\\ &-m_1e_2(\hat{x}_2-(\eta_2+m_1x_1)^{\frac{l_2}{l_1}})-m_1e_2^2.\end{aligned} \tag{32}$$

Next, the remaining term in (32) will be dealt. We firstly deal with the first term of the right hand of Eq.32.

According to the homogeneity of u,

$$|u(\hat{x})|\leq c||\hat{x}||_{\Delta_x}^{l_2+\tau}\leq c||x||_{\Delta_x}^{l_2+\tau}+c||e||_{\Delta_x}^{l_2+\tau} \tag{33}$$

where $||\hat{x}||_{\Delta_x}=(|\hat{x}_1|^{\frac{2}{l_1}}+|\hat{x}_2|^{\frac{2}{l_2}})^{1/2}$, $\Delta_x=(l_1,l_2)$. By the definition of homogeneous norm,

$$\begin{aligned}||x||_{\Delta_x}&=(|\xi_1^{2/l_1}+|\xi_2-\alpha_1\xi_1^{l_2/l_1}|^{2/l_2})^{1/2}\\ &\leq c(|\xi_1|^{2/l_1}+|\xi_2|^{2/l_2})^{1/2}\\ &=c||\xi||_{\Delta_x}.\end{aligned} \tag{34}$$

Therefore,

$$|u(\hat{x})|\leq c||\xi||_{\Delta_x}^{l_2+\tau}+c||e||_{\Delta_x}^{l_2+\tau}. \tag{35}$$

Then

$$\begin{aligned}&u(\hat{x})(x_2^{\frac{l_1}{l_2}}-(\eta_2+m_1x_1))\\ &\leq c(||\xi||_{\Delta_x}^{l_2+\tau}+||e||_{\Delta_x}^{l_2+\tau})(c|e_2|^{\frac{l_1}{l_2}}+m_1|e_1|)\\ &\leq\frac{1}{8}(\xi_1^{2l_2/l_1}+\xi_2^2)+\tilde{h}_1e_2^2,\end{aligned} \tag{36}$$

where $\tilde{h}_1$ is a constant.

Now we deal with the second term of the right hand of Eq.32. By Lemma 6, one obtains

$$\begin{aligned}&-m_1e_2(\hat{x}_2-(\eta_2+m_1x_1)^{\frac{l_2}{l_1}})\\ &\leq cm_1^2|e_2e_1|\times|x_2^{\frac{l_2-l_1}{l_2}}+e_2^{\frac{l_2-l_1}{l_2}}+[m_1e_1]^{\frac{l_2}{l_1}-1}|\\ &\leq c|e_1|m_1^2|e_2||\xi_2^{\frac{l_2-l_1}{l_2}}+c\xi_1^{\frac{l_2-l_1}{l_1}}+e_2^{\frac{l_2-l_1}{l_2}}+[m_1e_1]^{\frac{l_2}{l_1}-1}|.\end{aligned} \tag{37}$$

Via Young's inequality, one can get

$$-m_1e_2(\hat{x}_2-(\eta_2+m_1x_1)^{\frac{l_2}{l_1}})\leq e_2^2+\frac{1}{16}(\xi_2^2+\xi_1^{\frac{2l_2}{l_1}}), \tag{38}$$

where h_3 is a constant.

According to (36) and (38), the derivative of U can be rewritten as

$$\dot{U}=\frac{1}{2}(\xi_1^{\frac{2l_2}{l_1}}+\xi_2^2)-(m_1-1-\tilde{h}_1)e_2^2. \tag{39}$$

Because the state variable x_2 is not measurable, controller (12) results in a redundant term $\xi_2^{(2l_2-\tau)/(l_2-1)}(u-u^*)$ in (25) which is dealt as follows.

Because u is a C^1 function,

$$u(\hat{x})-u^*(x)=e_2\int_0^1\left.\frac{\partial u(X)}{\partial(X)}\right|_{X=x-\lambda e}d\lambda. \tag{40}$$

According to the homogeneity of $u^*(x)$ whose degree is $l_2+\tau$, so $\frac{\partial u(X)}{\partial(X)}$ is homogeneous of degree τ. It can be known from equation (34) that

$$\left.\frac{\partial u(X)}{\partial(X)}\right|_{X=x-\lambda e}\leq c||\xi||_{\Delta_x}^{\tau}+c||e||_{\Delta_x}^{\tau}. \tag{41}$$

According to Yang's inequality,

$$\xi_2^{\frac{2l_2-\tau}{l_2}-1}(u^*(\hat{x})-u(x))\leq\frac{1}{4}(\xi_1^{\frac{2l_2}{l_1}}+\xi_2^2)+\tilde{h}_2e_2^2, \tag{42}$$

where $\tilde{h}_2\geq 0$.

We construct a Lyapunov function for the system (19) as

$$W=U+V_2. \tag{43}$$

Combing (25), (39) and (42), the derivative of W is

$$\dot{W}\leq-\frac{1}{4}\sum_{i=1}^{2}\xi_i^{\frac{2l_2}{l_i}}-(m_1-1-\tilde{h}_2-\tilde{h}_1)e_2^2. \tag{44}$$

It is obvious that if one selects

$$m_1=\frac{1}{4}+1+\tilde{h}_2+\tilde{h}_1, \tag{45}$$

(44) becomes

$$\dot{W}\leq-\frac{1}{4}(\xi_1^{\frac{2l_2}{l_1}}+\xi_2^2+e_2^2). \tag{46}$$

Define

$$X=(x_1,x_2,\eta_2)^T. \tag{47}$$

It is obvious that the right hand side of the equation (46) is negative definite, so it can be proved that the system (19) is asymptotically stable under the controller and observer designed in this chapter. Meanwhile, the closed-loop system (19), observer (11) and controller (12) are rewritten as the following form

$$\dot{X} = F(X) = (x_2, u(\hat{x}), \dot{\eta}_2)^T, \tag{48}$$

which is homogeneous of degree τ.

According to lemma 3, the equation (44) can be rewritten as

$$\frac{\partial W(X)}{\partial X} \leq -c_1 ||X||_{\Delta}^{2l_2}. \tag{49}$$

Next, we will prove that the lateral stability control system of EV-DFIM (9) can also be asymptotically stable under the controller (12) and observer (11) based on the aforementioned proof.

Firstly, coordinate transformation is carried out for system (9). Then $z_1 = x_1$, $z_2 = \frac{x_2}{L}$, $u(\hat{z}) = \frac{u(\hat{x})}{L^2}$ with $L \geq 1$, then the system (9) becomes

$$\begin{aligned} \dot{z}_1 &= Lz_2 + \phi_1(t, z, u(\hat{z}), d(t)) \\ \dot{z}_2 &= Lu(\hat{z}) + \frac{\phi_2(t, z, u(\hat{z}), d(t))}{L} \\ y(t) &= z_1(t). \end{aligned} \tag{50}$$

Adopting the same Lyapunov function $W(X)$, it can be obtained that the derivative of Lyapunov of equation(50) is

$$\begin{aligned} \dot{W}_f &\leq -\frac{1}{4}(\xi_1^{2l_2/l_1} + \xi_2^2 + e_2^2) + \frac{\partial W_f(Z)}{\partial Z}(\phi_1, \frac{\phi_2}{L}, 0)^T \\ &\leq -Lc_1 ||Z||_{\Delta}^{2l_2} + \frac{\partial W_f(Z)}{\partial Z}(\phi_1, \frac{\phi_2}{L}, 0)^T. \end{aligned} \tag{51}$$

According to Assumption 1, one gets

$$\begin{aligned} &|\phi_1(t, z, u(\hat{z}))| \leq c|z_1|^{\frac{l_1+\tau}{l_1}} \\ &|\frac{\phi_2(t, z, u(\hat{z}))}{L}| \leq cL^{1-\frac{1}{\tau+1}}(|z_1|^{\frac{l_2+\tau}{l_1}} + |z_2|^{\frac{l_2+\tau}{l_2}}). \end{aligned} \tag{52}$$

$\frac{\partial W_f(Y)}{\partial Z_i}$ is homogeneous of degree $2l_2 - \tau - l_i, i = 1, 2$. According to Lemma 2, one knows that

$$\begin{aligned} &|\frac{\partial W_f(Z)}{\partial Z_1}|(|z_1|^{\frac{l_1+\tau}{l_1}}) \\ &|\frac{\partial W_f(Z)}{\partial Z_2}|(|z_1|^{\frac{l_2+\tau}{l_1}} + |z_2|^{\frac{l_2+\tau}{l_2}}) \end{aligned} \tag{53}$$

is homogeneous of degree $2l_2$.

With (52) and equation (53), there exists a constant χ_i such that

$$\frac{\partial W_f(Z)}{\partial Z_i}\frac{\phi_i(z)}{L^{i-1}} \leq \chi_i L^{1-\frac{1}{(i-1)\tau+1}} ||Z||_{\Delta}^{2l_2}. \tag{54}$$

Substitute (54) into (51) yields

$$\dot{W}_f \leq -L(c_1 - \sum_{i=1}^{2} \chi_i L^{-\frac{1}{(i-1)\tau+1}}) ||Z||_{\Delta}^{2l_2}. \tag{55}$$

It is obvious that if L is large enough the right hand side of (55) is negative definite. That is to say, the system (9) can be globally asymptotically stabilized by the designed observer (11) and controller (12).

Proof ends.

IV. DESIGN OF YAW MOMENT DISTRIBUTION STRATEGY

The designed homogeneous domination controller calculates the yaw moment needed to stabilize the vehicle body. But in fact, the yaw moment is generated by the four in-whee motors of the IEV-DFIM. Therefore, it is necessary to coordinate the distribution of the driving torque of the four in-wheel motors. In this section, a direct yaw moment distribution strategy is designed based on an optimal allocation algorithm for the minimum adhesion coefficient utilization of tires.

For minimum adhesion coefficient utilization of tire, the objective function is constructed as

$$\min J = \frac{(F_{x_1})^2}{(\mu_1 F_{z_1})^2} + \frac{(F_{x_2})^2}{(\mu_2 F_{z_2})^2} + \frac{(F_{x_3})^2}{(\mu_3 F_{z_3})^2} + \frac{(F_{x_4})^2}{(\mu_4 F_{z_4})^2}. \tag{56}$$

In (56), $F_{x_1}, F_{x_2}, F_{x_3}, F_{x_4}$ are the longitudinal forces of the left front wheel, right front wheel, left rear wheel and right rear wheel respectively. F_{z_1}, F_{z_2}, F_{z_3}, F_{z_4} are the vertical forces of the left front wheel, right front wheel, left rear wheel, and right rear wheel respectively. $\mu_1, \mu_2, \mu_3, \mu_4$ are the adhesion coefficients of the left front wheel, right front wheel, left rear wheel, and right rear wheel respectively.

As the aforementioned information, the controller output should be the torque sum of four tire longitudinal forces. Therefore, we need to obtain the longitudinal forces of four tires. According to vehicle dynamics, there exists

$$F_t = F_f + F_w + F_i + F_j, \tag{57}$$

where F_t is the total vehicle driving force, F_f is the rolling resistance, F_w is the air resistance, F_i is the grade resistance, F_j is the acceleration resistance. For analysis convenience, It is assumed that the vehicle runs at a constant speed on a horizontal road, i.e., $F_i = 0$, $F_j = 0$, then the driving force equation can be expressed as

$$F_t = (Gf + \frac{C_D A v_x^2}{21.15}) = F_{x_1} + F_{x_2} + F_{x_3} + F_{x_4}, \tag{58}$$

where G is the vehicle gravity, f is the coefficient of rolling resistance, C_D is the coefficient of air resistance, A is the windage area, v_x is the vehicle speed.

Then the needed yaw moment T_z can be calculated by

$$T_z = \frac{d}{2}(-F_{x_1} + F_{x_2} - F_{x_3} + F_{x_4}), \tag{59}$$

where d is the wheel distance. By (58) and equation (59), one gets

$$\begin{aligned} F_{x_3} &= (0.5Gf + \frac{C_D A v_x^2}{42.3} - \frac{1}{d}T_z - F_{x_1}) \\ F_{x_4} &= (0.5Gf + \frac{C_D A v_x^2}{42.3} + \frac{1}{d}T_z - F_{x_2}). \end{aligned} \tag{60}$$

TABLE 1. Vehicle parameters.

Vehicle Parameters	Nominal Value	Unit
Vehicle mass	1274	kg
Axle distance	2478	mm
Front wheel distance	1550	mm
Rear wheel distance	1550	mm
Distance between the front axle and centroid	1016	mm
Distance between the rear axle and centroid	1462	mm
Height of center of mass	540	mm
Rotational inertia	1523	$N{\cdot}m^2$
Cornering stiffness of front wheels	-53000	N/rad
Cornering stiffness of rear wheels	-53000	N/rad

TABLE 2. Parameters of two controllers in numerical simulation.

Homogeneous Controller	Nominal Value	Sliding Mode Controller	Nominal Value
l_1	1.89	C_1	0.11
l_2	2.15	C_2	0.10
τ	0.01	k_1	2.89
γ_1	1.03	k_2	3.14
γ_2	1.31	ϵ	0.10
n_1	0.85	Q	137
m_1	7.4		

Substitute (60) into (57), the derivatives of J with respect to F_{x_1} and F_{x_2} are

$$\frac{\partial J}{\partial F_{x_1}} = \frac{1}{u^2}\left(\frac{2F_{x_1}}{F_{z_1}^2} - \frac{Gf + \frac{C_D A {v_x}^2}{21.15} - \frac{2}{d}T_z - 2F_{x_1}}{F_{z_3}^2}\right) = 0 \quad (61)$$

$$\frac{\partial J}{\partial F_{x_2}} = \frac{1}{u^2}\left(\frac{2F_{x_2}}{F_{z_2}^2} - \frac{Gf + \frac{C_D A {v_x}^2}{21.15} - \frac{2}{d}T_z - 2F_{x_2}}{F_{z_4}^2}\right) = 0 \quad (62)$$

Then we can obtain the longitudinal forces of every wheel, i.e., the needed torques of every in-wheel motor are obtained.

V. SIMULATION AND ANALYSIS

In this section, the numerical simulations are carried out to verify the efficiency of the designed homogeneous domination-based observer and controller under three working conditions with 80km/h and 120km/h respectively compared with the sliding mode controller. The disturbance $sin(2\pi t)/(1+t^3)$ is adopted. The vehicle parameters used are shown in Tab.1, and the simulation parameters of the controller are shown in Tab.2.

A. NUMERICAL SIMULATION UNDER 80km/H

Under 80km/h, the yaw rate with the homogeneous domination controller and sliding mode controller is shown in Fig.2. From which one can find that the maximum oscillation value is about 0.106rad/s with the homogeneous domination controller. After 0.9s, the oscillation value of the wave peak is about 0.089rad/s, and then tends to be stable rapidly, and reaches zero after 2.3s. By contrast, the yaw rate with the sliding mode controller, the maximum oscillating value is as high as 0.26rad/s. After 0.92s, the oscillation value of the wave peak is still 0.126rad/s. Subsequently, the oscillation tends to be stable and reaches zero after 4s.

As shown in Fig.3, the maximum oscillating value of the side slip angle is only 0.212rad with the homogeneous

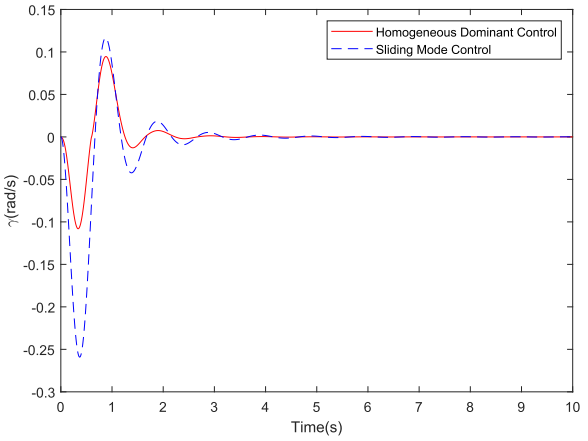

FIGURE 2. The yaw rate with the homogeneous domination controller and sliding mode controller under 80km/h.

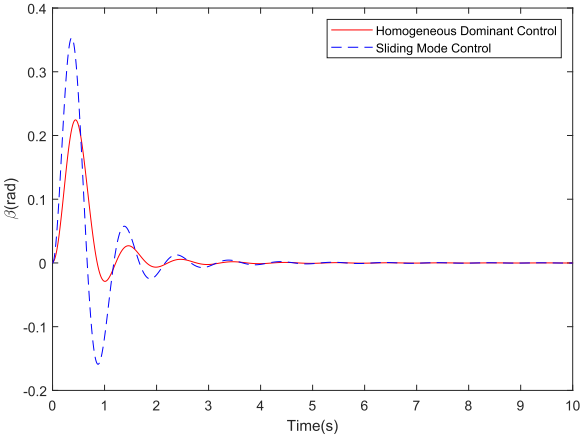

FIGURE 3. The side slip angle with the homogeneous domination controller and sliding mode controller under 80km/h.

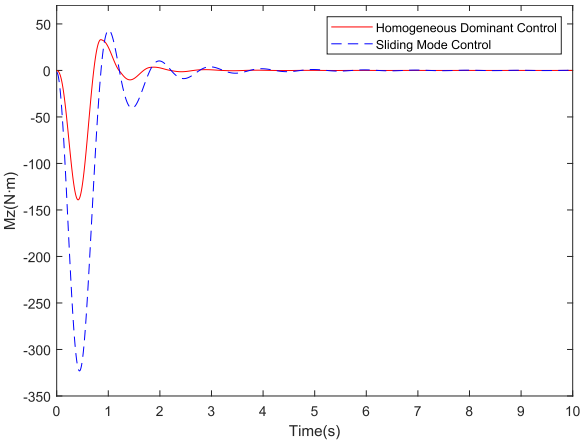

FIGURE 4. The yaw moment with the homogeneous domination controller and sliding mode controller under 80km/h.

domination controller. After 1s, the oscillation value rapidly converges to zero and reaches zero after 3s. For the sliding mode controller, the maximum side slip angle is as high as 0.361rad. After 0.95s, the oscillation value of the peak is still 0.156rad. It tends to be zero after 4.5s.

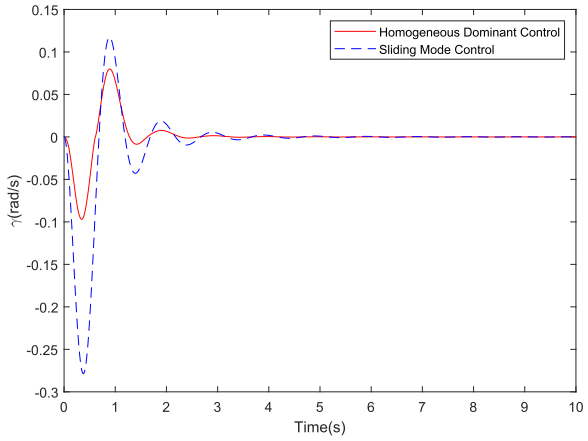

FIGURE 5. The yaw rate with the homogeneous domination controller and sliding mode controller under 120km/h.

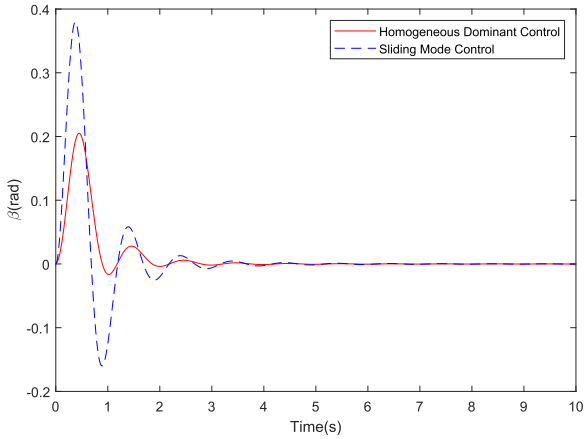

FIGURE 6. The side slip angle with the homogeneous domination controller and sliding mode controller under 120km/h.

As shown in Fig.4, the homogeneous domination controller just outputs maximum value 140N·m to meet the stability requirement, then decreases the output rapidly. After 2.1s, the vehicle is stabilized completely. By contrast, the sliding mode controller needs to output maximum 325N·m to meet the requirement. And the vehicle is stabilized to zero after 4s. This means the sliding mode controller should output more energy and time to stabilize the vehicle than the homogeneous domination controller.

B. NUMERICAL SIMULATION UNDER 120km/H

Fig.5 shows that the maximum oscillation value is only 0.08rad/s with the homogeneous domination controller. The yaw rate tends to zero after 2.2s. However, the maximum oscillation value is about 0.275rad/s with the sliding mode controller and tends to zero after 4s.

As shown in Fig.6, the maximum oscillation value of the side slip angle with the homogeneous domination controller is 0.21rad. Then the side slip angle quickly tends to be zero. The oscillation peak with the sliding mode controller is up to 0.38rad. Followed by several oscillation peaks, the side slip angle tends to zero.

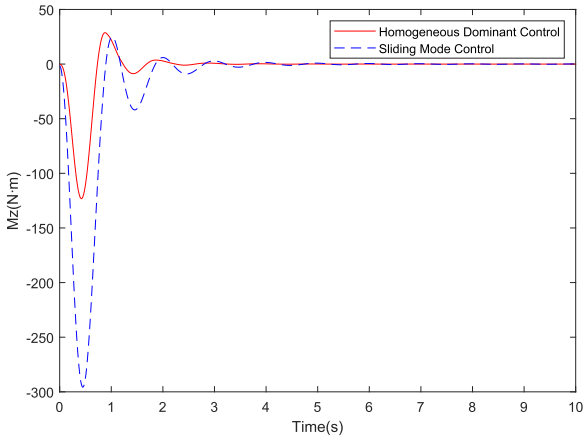

FIGURE 7. The yaw moment with the homogeneous domination controller and sliding mode controller under 120km/h.

Fig.7 shows that the sliding mode controller outputs the maximum yaw moment is up to 300N·m and stabilizes the vehicle after 4.5s. While the homogeneous domination controller just outputs 120N·m and stabilizes the vehicle after 2.1s. It can be seen that the torque requirement of homogeneous dominant control is much smaller than the sliding mode controller, and the homogeneous domination controller has a better control effect than the sliding mode controller.

According to the above simulation analysis, it is concluded that compared with the sliding mode controller, the homogeneous domination controller has better control effects for the yaw rate, side slip angle, and control output. On the other hand, it is obvious that the homogeneous domination controller has strong robustness which is more suitable for the lane keeping system.

VI. HARDWARE-IN-LOOP SIMULATION ANALYSIS

The Hardware-in-loop (HIL) simulation system is composed of a MicroAutoBox (dSPACE), Lenovo Legion laptop (CPU Intel i7-11800H, GPU NVIDIA RTX3060, RAM DDR4 2666), Matlab, and CarSim software. The designed control algorithm is programmed by Matlab and inputted into MicroAutoBox. MicroAutoBox acquires the necessary signals from the driverless car and outputs control orders to four in-wheel motors according to the designed control algorithm. At the same time, MicroAutoBox transfers the car status to CarSim. The HIL simulation system communicates via the CAN bus. And the control period is set to 100ms. The ControlDesk module of CarSim monitors and records the car's running data. Then CarSim displays the car status via real-time animation. HIL simulation is carried out under straight road condition with a speed of 80km/h. In the simulation, the IEV-DFIM runs along the center line of the lane controlled by the lane keeping system. The lateral stability control system will work if the lane keeping system may cause the IEV-DFIM to reach the lateral stability limit. The homogeneous domination method still is simulated compared with the sliding mode control method. The simulated IEV-DFIM's

TABLE 3. Two controllers' parameters in HIL simulation.

Homogeneous Controller Parameters	Nominal Value	Sliding Mode Controller Parameters	Nominal Value
l_1	1.37	c_1	1.23
l_2	3.19	c_2	0.45
τ	0.01	k_r	0.11
γ_1	1.04	k_1	3.24
γ_2	1.15	ϵ	0.10
k_1	0.96	Q	154
m_1	5.37		

(a) The MicroAutoBox

(b) The driverless car

(c) The simulation display interface

FIGURE 8. The hardware-in-loop simulation system.

parameters are shown in Tab.1, and the two controllers' parameters are shown in Tab.3. The HIL simulation system is shown in Fig. 8.

Remark 2: Some parameters of the controller are the coefficients of Hurwitz poly-nomial and others are selected via our experience. The dynamic model used in the numerical simulation is Eq.1 which is a simplified 2DOF model. But the dynamic model used in the HIL simulation is a vehicle dynamic model provided by the CarSim software which includes all the subsystems of the vehicle. The different dynamic models need different parameters of the controller. Therefore, the controller parameters used in the numerical simulation at 80km/h are different from the controller parameters used in the HIL simulation at the same 80km/h.

As shown in Fig.9, with the homogeneous domination controller, the yaw rate of the vehicle reaches the maximum value 0.14rad/s at 2.3s and tends to zero at 5.5s. The practical curve is close to the desired yaw rate curve throughout the whole process. By contrast, the yaw rate reaches the maximum value 0.18rad/s at 2.3s and tends to zero at 5.5s with the sliding mode controller. The deviation between the practical curve and desired curve is larger, and the practical curve is close to the desired curve at 4.3s.

As shown in Fig.10, with the homogeneous domination controller, the side slip angle reaches the maximum value

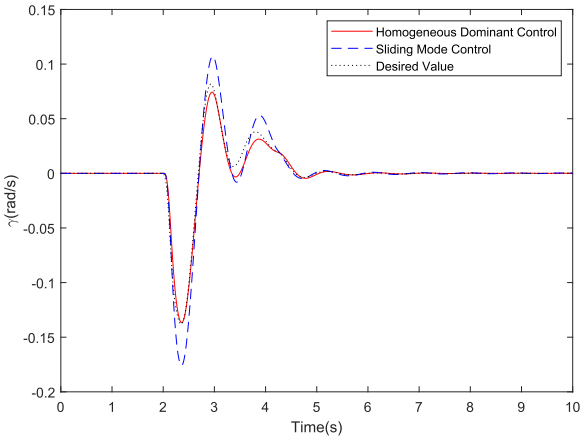

FIGURE 9. The yaw rate of the car running on the straight lane with the homogeneous domination controller and sliding mode controller under 80km/h.

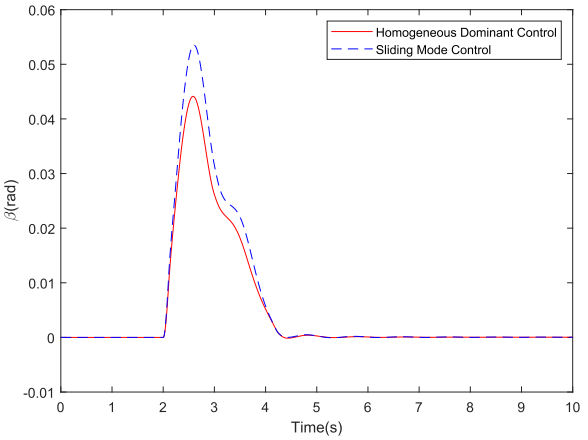

FIGURE 10. The side slip angle of the car running on the straight lane angle with the homogeneous domination controller and sliding mode controller under 80km/h.

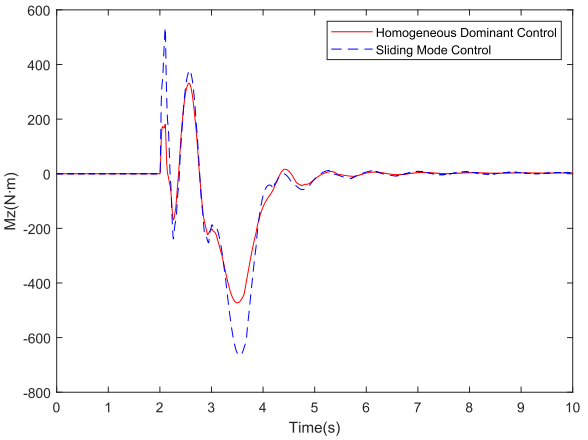

FIGURE 11. The yaw moment of the car running on the straight lane with the homogeneous domination controller and sliding mode controller under 80km/h.

0.044rad at 2.3s and tends to zero at 4.2s. In contrast, the side slip angle with the sliding mode controller reaches 0.055rad at 2.4s, which is larger than the homogeneous domination controller, and tends to zero at 4.2s.

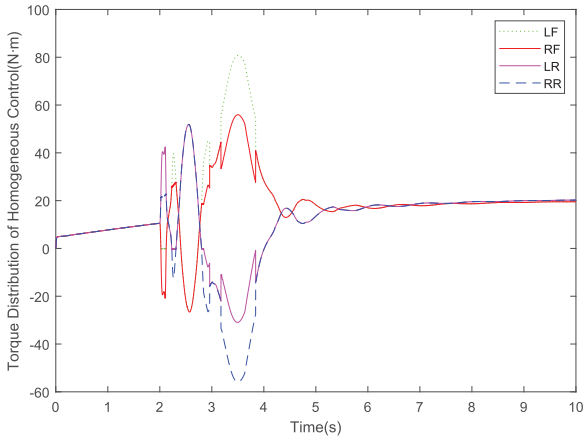

FIGURE 12. The torque distribution of the car running on the straight lane with the homogeneous domination controller under 80km/h.

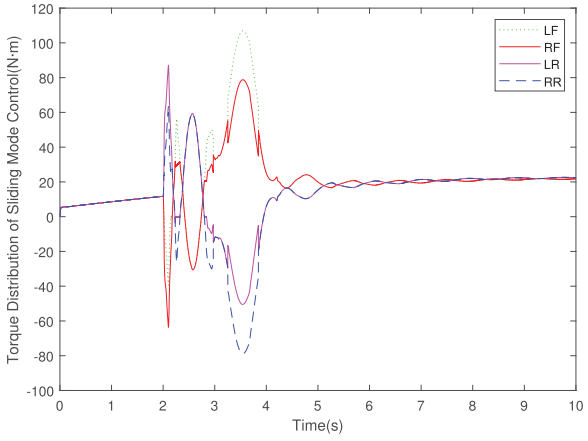

FIGURE 13. The torque distribution of the car running on the straight lane with sliding mode controller under 80km/h.

Fig.11 shows that the yaw moment maximum value needs to be 520 N·m with the homogeneous domination controller. But the yaw moment maximum value needs to be 680 N·m with the sliding mode controller.

Fig.12 and Fig.13 show that each in-wheel motor needs smaller torque output with the homogeneous domination controller than the sliding mode controller.

In conclusion, we can get that the homogeneous domination controller has a better control effect than the sliding mode controller, and is more suitable for engineering applications. The homogeneous domination controller can improve the IEV-DFIM's lateral stability for safety when the lane keeping system is working.

VII. CONCLUSION

To improve the IEV-DFIM's lateral stability for lane keeping system, the homogeneous domination control method is proposed. The two-degree-of-freedom dynamic model of an IEV-DFIM for lateral stability is constructed. Based on the established dynamics equations, the state equation of the IEV-DFIM stability control system is obtained, and the homogeneous domination observer and controller are designed based on the homogeneous theory. The Lyapunov method is used to prove that the designed observer and controller can globally asymptotically stabilize the nonlinear system. The numerical simulation and HIL simulation are carried out. The results show that the homogeneous domination controller has better control effects on yaw rate and side slip angle compared with the classical sliding mode controller, and the controller output is obviously smaller than the classical sliding mode controller which reduces the requirement for the physical controller and the energy consumption.

REFERENCES

[1] H. Wang, W. Cui, Z. Xia, and W. Jiang, "Vehicle lane keeping system based on TSK fuzzy extension control," *Proc. Inst. Mech. Eng., D, J. Automobile Eng.*, vol. 234, nos. 2–3, 2019, Art. no. 09544070198492 5.

[2] M. Karthikeyan, S. Sathiamoorthy, and M. Vasudevan, "Lane keep assist system for an autonomous vehicle using support vector machine learning algorithm," in *Proc. Int. Conf. Innov. Data Commun. Technol. Appl.* Cham, Switzerland: Springer, 2020, pp. 101–108.

[3] F. Tahami, R. Kazemi, and S. Farhanghi, "A novel driver assist stability system for all-wheel-drive electric vehicles," *IEEE Trans. Veh. Technol.*, vol. 52, no. 3, pp. 683–692, May 2003.

[4] Q. Meng, Z.-Y. Sun, and Y. Li, "Finite-time controller design for four-wheel-steering of electric vehicle driven by four in-wheel motors," *Int. J. Control, Autom. Syst.*, vol. 16, no. 4, pp. 1814–1823, Aug. 2018.

[5] H. Wang, C. Hu, W. Cui, and H. Du, "Multi-objective comprehensive control of trajectory tracking for four-in-wheel-motor drive electric vehicle with differential steering," *IEEE Access*, vol. 9, pp. 62137–62154, 2021.

[6] Z. Wang, J. Shao, and Z. He, "Fault tolerant sensorless control strategy with multi-states switching method for in-wheel electric vehicle," *IEEE Access*, vol. 9, pp. 61150–61158, 2021.

[7] Y. Jeong and S. Yim, "Path tracking control with four-wheel independent steering, driving and braking systems for autonomous electric vehicles," *IEEE Access*, vol. 10, pp. 74733–74746, 2022.

[8] S. Ding and J. Sun, "Direct yaw-moment control for 4WID electric vehicle via finite-time control technique," *Nonlinear Dyn.*, vol. 88, no. 1, pp. 1–16, 2016.

[9] Z. Zhao and D. Ronghua, "Yaw moment control strategy for four wheel side driven EV," *Autom. Control Comput. Sci.*, vol. 52, no. 1, pp. 32–39, Jan. 2018.

[10] E. Joa, K. Yi, K. Sohn, and H. Bae, "Four-wheel independent brake control to limit tire slip under unknown road conditions," *Control Eng. Pract.*, vol. 76, pp. 79–95, Jul. 2018.

[11] X. He, Y. Liu, K. Yang, J. Wu, and X. Ji, "Robust coordination control of AFS and ARS for autonomous vehicle path tracking and stability," in *Proc. IEEE Int. Conf. Mechatronics Autom. (ICMA)*, Aug. 2018, pp. 924–929.

[12] T. Chen, L. Chen, X. Xu, Y. Cai, and X. Sun, "Simultaneous path following and lateral stability control of 4WD–4WS autonomous electric vehicles with actuator saturation," *Adv. Eng. Softw.*, vol. 128, pp. 46–54, Feb. 2019.

[13] C. Zhang, R. Zhang, R. Wang, B. Chang, and J. Ma, "Design of torque distribution strategy for four-wheel-independent-drive electric vehicle," *Autom. Control Comput. Sci.*, vol. 54, no. 6, pp. 501–512, Nov. 2020.

[14] A.-T. Nguyen, P. Chevrel, and F. Claveau, "LPV static output feedback for constrained direct tilt control of narrow tilting vehicles," *IEEE Trans. Control Syst. Technol.*, vol. 28, no. 2, pp. 661–670, Mar. 2020.

[15] Z. Li, P. Wang, H. Liu, Y. Hu, and H. Chen, "Coordinated longitudinal and lateral vehicle stability control based on the combined-slip tire model in the MPC framework," *Mech. Syst. Signal Process.*, vol. 161, Dec. 2021, Art. no. 107947.

[16] C. Jing, H. Shu, R. Shu, and Y. Song, "Integrated control of electric vehicles based on active front steering and model predictive control," *Control Eng. Pract.*, vol. 121, Apr. 2022, Art. no. 105066.

[17] Q. Meng, T. Zhao, C. Qian, Z. Y. Sun, and P. Ge, "Integrated stability control of AFS and DYC for electric vehicle based on non-smooth control," *Int. J. Syst. Sci.*, vol. 49, nos. 5–8, pp. 1–11, 2018.

[18] Q. Meng, H. Xu, and Z.-Y. Sun, "Nonlinear lateral motion stability control method for electric vehicle based on the combination of dual extended state observer and domination approach via sampled-data output feedback," *Trans. Inst. Meas. Control*, vol. 43, no. 10, pp. 2258–2271, Jun. 2021.

[19] C. Qian and J. Li, "Global output feedback stabilization of upper-triangular nonlinear systems using a homogeneous domination approach," *Int. J. Robust Nonlinear Control*, vol. 16, pp. 441–463, Jun. 2006.
[20] X.-J. Xie and L. Liu, "A homogeneous domination approach to state feedback of stochastic high-order nonlinear systems with time-varying delay," *IEEE Trans. Autom. Control*, vol. 58, no. 2, pp. 494–499, Feb. 2013.
[21] C.-C. Chen and S. S.-D. Xu, "Global stabilization for a class of genuinely nonlinear systems with a time-varying power: An interval homogeneous domination approach," *IEEE Access*, vol. 6, pp. 11255–11264, 2018.
[22] C. Qian, "A homogeneous domination approach for global output feedback stabilization of a class of nonlinear systems," in *Proc. Amer. Control Conf.*, 2005, pp. 4708–4715.
[23] J. Li, C. Qian, and S. Ding, "Global finite-time stabilisation by output feedback for a class of uncertain nonlinear systems," *Int. J. Control*, vol. 83, no. 11, pp. 2241–2252, 2010.
[24] J.-Y. Zhai, "Decentralised output-feedback control for a class of stochastic non-linear systems using homogeneous domination approach," *IET Control Theory Appl.*, vol. 7, no. 8, pp. 1098–1109, May 2013.
[25] L. Chai and C. Qian, "Global stabilization via homogeneous output feedback for a class of uncertain nonlinear systems subject to time delays," *Trans. Inst. Meas. Control*, vol. 36, no. 4, pp. 478–486, Jun. 2014.
[26] H. Du, C. Qian, S. Li, and Z. Chu, "Global sampled-data output feedback stabilization for a class of uncertain nonlinear systems," *Automatica*, vol. 99, pp. 403–411, Jan. 2019.
[27] J. Zhu and C. Qian, "Local asymptotic stabilization for a class of uncertain upper-triangular systems," *Automatica*, vol. 118, Aug. 2020, Art. no. 108954.
[28] K. Cao and C. Qian, "Finite-time controllers for a class of planar nonlinear systems with mismatched disturbances," *IEEE Control Syst. Lett.*, vol. 5, no. 6, pp. 1928–1933, Dec. 2021.
[29] Q. Meng, C. Qian, Z.-Y. Sun, and C.-C. Chen, "A homogeneous domination output feedback control method for active suspension of intelligent electric vehicle," *Nonlinear Dyn.*, vol. 103, no. 2, pp. 1627–1644, Jan. 2021.
[30] G. Zhao, Z.-G. Su, Z.-Y. Sun, and Y. Sun, "Homogeneous domination control for uncertain nonlinear systems via interval homogeneity with monotone degrees," *IEEE Access*, vol. 8, pp. 48632–48641, 2020.
[31] Y. Jiang and J. Zhai, "Practical tracking control for a class of high-order switched nonlinear systems with quantized input," *ISA Trans.*, vol. 96, pp. 218–227, Jan. 2020.
[32] A. Lx, B. Zl, and C. Wz, "Decentralized tracking control for a class of stochastic high-order time-delay nonlinear systems under arbitrary switchings," *J. Franklin Inst.*, vol. 357, no. 2, pp. 887–905, 2020.
[33] K. Alimhan, O. J. Mamyrbayev, G. A. Abdenova, and A. Akmetkalyeva, "Output tracking control for high-order nonlinear systems with time delay via output feedback design," *Symmetry*, vol. 13, no. 4, p. 675, Apr. 2021.
[34] Y. Liu, Y. Li, and W. Li, "Output-feedback stabilization of a class of stochastic nonlinear systems with time-varying powers," *Int. J. Robust Nonlinear Control*, vol. 31, no. 18, pp. 9175–9192, 2021.
[35] Z. Liu, Y. Tian, and Z. Sun, "An adaptive homogeneous domination method to time-varying control of nonlinear systems," *Int. J. Robust Nonlinear Control*, vol. 32, no. 1, pp. 527–540, Jan. 2022.
[36] Z. Y. Sun, C. Liu, S. F. Su, and W. Sun, "Global finite-time stabilization for uncertain systems with unknown measurement sensitivity," *IEEE Trans. Cybern.*, vol. 52, no. 8, pp. 7602–7611, Aug. 2022.
[37] Q. Meng, C. Qian, and P. Wang, "Lateral motion stability control via sampled-data output feedback of a high-speed electric vehicle driven by four in-wheel motors," *J. Dyn. Syst., Meas., Control*, vol. 140, no. 1, Jan. 2018, Art. no. 011002.
[38] M. Kawski, "Homogeneous stabilizing feedback laws," *Control Theory Adv. Technol.*, vol. 6, no. 4, pp. 497–516, 1990.
[39] H. Hermes, "Homogeneous coordinates and continuous asymptotically stabilizing feedback controls," *Differ. Equ., Stability, Control*, vol. 109, no. 1, pp. 249–260, 1991.
[40] G. Hardy, J. Littlewood, and G. Polya, *Ainequalities*. Cambridge, U.K.: Cambridge Univ. Press, 1952.
[41] C. Qian and W. Lin, "A continuous feedback approach to global strong stabilization of nonlinear systems," *IEEE Trans. Autom. Control*, vol. 46, no. 7, pp. 1061–1079, Jul. 2001.

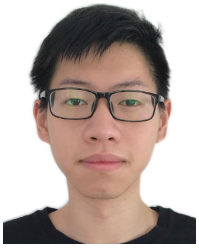

QIXIAN WANG received the bachelor's degree from Hangzhou Dianzi University, China, in 2021, where he is currently pursuing the graduate degree with the School of Mechanical Engineering. His current research interests include electric vehicle stability control and electric vehicle shimmy control.

QINGHUA MENG received the Ph.D. degree from Zhejiang University, China, in 2005. Since 2005, he has been with the School of Mechanical Engineering, Hangzhou Dianzi University, where he is a Professor. His current research interests include electric vehicle stability control, mechanical fault diagnosis, and signal processing.

LIDAN CHEN received the master's degree in mechanical and electrical engineering from the Zhejiang University of Technology, in 2008. Since 2005, he has been a Teacher with the School of Automotive Technology, Zhejiang Technical Institute of Economics. In 2013, he was appointed as a Professor of mechanical engineering. His research interests include vehicle fault diagnosis and intelligent and connected vehicle technology.

HAIBIN HE received the Ph.D. degree from Zhejiang University, China, in 2017. Currently, he is working with Hangzhou Dianzi University, where he is an Associate Research Fellow. His current interests include control system design, mechanical fault diagnosis, and signal processing.